



Plasma BDNF Levels Following Transcranial Direct Current Stimulation Allow Prediction of Synaptic Plasticity and Memory Deficits in 3 × Tg-AD Mice

OPEN ACCESS

Edited by:

Stylianos Kosmidis,
Columbia University, United States

Reviewed by:

Tangui Maurice,
INSERM U1198 Mécanismes
Moléculaires dans les Démences
Neurodégénératives, France
Kei Cho,
King's College London,
United Kingdom
Victor Luna,
Columbia University Irving Medical
Center, United States

*Correspondence:

Maria Vittoria Podda
maria.vittoria.podda@unicatt.it
Claudio Grassi
claudio.grassi@unicatt.it

Specialty section:

This article was submitted to
Molecular Medicine,
a section of the journal
Frontiers in Cell and Developmental
Biology

Received: 09 April 2020

Accepted: 09 June 2020

Published: xx June 2020

Citation:

Cocco S, Rinaudo M, Fusco S,
Longo V, Gironi K, Renna P,
Aceto G, Mastrodonato A,
Li Puma DD, Podda MV and
Grassi C (2020) Plasma BDNF Levels
Following Transcranial Direct Current
Stimulation Allow Prediction
of Synaptic Plasticity and Memory
Deficits in 3 × Tg-AD Mice.
Front. Cell Dev. Biol. 8:541.
doi: 10.3389/fcell.2020.00541

Sara Cocco¹, Marco Rinaudo¹, Salvatore Fusco^{1,2}, Valentina Longo¹, Katia Gironi¹, Pietro Renna¹, Giuseppe Aceto¹, Alessia Mastrodonato¹, Domenica Donatella Li Puma^{1,2}, Maria Vittoria Podda^{1,2*} and Claudio Grassi^{1,2*}

¹ Department of Neuroscience, Università Cattolica del Sacro Cuore, Rome, Italy, ² Fondazione Policlinico Universitario A. Gemelli IRCCS, Rome, Italy

Early diagnosis of Alzheimer's disease (AD) supposedly increases the effectiveness of therapeutic interventions. However, presently available diagnostic procedures are either invasive or require complex and expensive technologies, which cannot be applied at a larger scale to screen populations at risk of AD. We were looking for a biomarker allowing to unveil a dysfunction of molecular mechanisms, which underly synaptic plasticity and memory, before the AD phenotype is manifested and investigated the effects of transcranial direct current stimulation (tDCS) in 3 × Tg-AD mice, an experimental model of AD which does not exhibit any long-term potentiation (LTP) and memory deficits at the age of 3 months (3 × Tg-AD-3M). Our results demonstrated that tDCS differentially affected 3 × Tg-AD-3M and age-matched wild-type (WT) mice. While tDCS increased LTP at CA3-CA1 synapses and memory in WT mice, it failed to elicit these effects in 3 × Tg-AD-3M mice. Remarkably, 3 × Tg-AD-3M mice did not show the tDCS-dependent increases in pCREB^{Ser133} and pCaMKII^{Thr286}, which were found in WT mice. Of relevance, tDCS induced a significant increase of plasma BDNF levels in WT mice, which was not found in 3 × Tg-AD-3M mice. Collectively, our results showed that plasticity mechanisms are resistant to tDCS effects in the pre-AD stage. In particular, the lack of BDNF responsiveness to tDCS in 3 × Tg-AD-3M mice suggests that combining tDCS with dosages of plasma BDNF levels may provide an easy-to-detect and low-cost biomarker of covert impairment of synaptic plasticity mechanisms underlying memory, which could be clinically applicable. Testing proposed here might be useful to identify AD in its preclinical stage, allowing timely and, hopefully, more effective disease-modifying interventions.

Keywords: Alzheimer's disease, blood biomarkers, BDNF, neuroplasticity, personalized medicine, tDCS

INTRODUCTION

Alzheimer's disease (AD) is a progressive neurodegenerative disorder responsible for the most common form of dementia. To date, therapeutic interventions against AD failed most likely because of late treatment initiation, i.e., when brain function and structure are already irreversibly damaged. Several lines of evidence suggest that pathogenic mechanisms of AD may affect the brain in the dark for many years owing to the brain's ability to cope with failures exploiting the so-called "cognitive reserve." Compensatory mechanisms can stave off neurodegeneration symptoms maintaining memory encoding for long time, and exhaustion of such brain ability may mark AD onset (Merlo et al., 2019). Thus, one primary goal is to detect preclinical AD, inasmuch as therapeutic interventions may have a higher success probability. Furthermore, some signs and symptoms, which manifested at early AD stages (e.g., depressive and cognitive symptoms in the measure of semantic memory and conceptual formation), are sometimes not recognized and/or mistaken for symptoms of other pathologies (Bature et al., 2017). This further stresses the need of reliable disease biomarkers, which may help early AD diagnosis.

Cognitive decline in AD is linked to pathological accumulation of amyloid-beta ($A\beta$) and Tau proteins and their aggregation in brain regions which are essential for memory encoding and storage, such as the medial temporal lobe and related cortical areas (Serrano-Pozo et al., 2011; Bloom, 2014). Striking evidence from preclinical studies indicates that both $A\beta$ and Tau have detrimental effects on molecular machinery of synapses, ultimately leading to decreased hippocampal long-term potentiation (LTP), a cellular correlate of memory (Irvine et al., 2008; Kopeikina et al., 2012; Ripoli et al., 2014; Fa et al., 2016; Puzzo et al., 2017; Gulisano et al., 2018a,b). However, decreased synaptic plasticity, similarly, to memory impairment, is manifested when the pathology has already developed. Molecular pathways, underlying synaptic plasticity, potentially deregulated or vulnerable in the pre-symptomatic stage, might provide early biomarkers to predict the onset and/or progression of the disease.

Recent studies, including ours, have shown that molecular determinants of synaptic plasticity, including brain-derived neurotrophic factor (BDNF), phosphorylation of CREB at Ser133 (pCREB^{Ser133}), calcium-calmodulin kinase II (CaMKII) at Thr286 (pCaMKII^{Thr286}) and AMPA receptor GluA1 subunit at Ser831 (pGluA1^{Ser831}), are engaged and boosted by transcranial direct current stimulation (tDCS) – a non-invasive neuromodulatory technique – resulting in increased LTP and enhanced cognitive or motor functions, depending on the stimulated brain area (Ranieri et al., 2012; Rohan et al., 2015; Podda et al., 2016; Kim et al., 2017; Paciello et al., 2018; Stafford et al., 2018; Barbati et al., 2019; Yu et al., 2019; Kronberg et al., 2020).

We hypothesized that tDCS might differentially impact LTP and memory in 3 × Tg-AD mice, a common model of AD, at a stage when the AD phenotype is not manifested yet (i.e., at 3 months of age, hereinafter referred to as 3 × Tg-AD-3M mice)

(Oddo et al., 2003; Stover et al., 2015; Belfiore et al., 2019), thus unveiling early dysfunction of synaptic plasticity mechanisms.

We found that tDCS failed to enhance LTP at CA3-CA1 synapses and memory in 3 × Tg-AD-3M mice whereas it increased these parameters in age-matched wild-type (WT) mice. Of note, 3 × Tg-AD-3M mice did not show increased pCREB^{Ser133}, pCaMKII^{Thr286}, and BDNF following tDCS, suggesting that these molecular changes could serve as novel early biomarkers for AD. Remarkably, BDNF responsiveness to tDCS was assessed in blood samples, providing an easy-to-detect and low-cost biomarker.

MATERIALS AND METHODS

Animals

Data of male triple transgenic AD (3 × Tg-AD) mice, harboring the Swedish human APP, presenilin M146V and tauP301L mutations (Oddo et al., 2003) were compared to C57BL/6 wild-type (WT) mice (Li et al., 2018; Chakroborty et al., 2019; Joseph et al., 2019). The colonies were established in-house at the Animal Facility of the Università Cattolica from breeding pairs purchased from the Jackson Laboratory. The study was performed on 3-month-old (3M) 3 × Tg-AD and WT mice ($n = 78$ and $n = 88$, respectively). Seven-month-old (7M) 3 × Tg-AD mice and age-matched WT mice ($n = 21$ each group) were also tested to validate the time course of AD phenotype in terms of synaptic plasticity and memory impairment in our experimental conditions. The animals were housed under a 12 h light-dark cycle at a controlled temperature (22–23°C) and constant humidity (60–75%).

Ethics Statement

All animal procedures were approved by the Ethics Committee of the Catholic University and were fully compliant with guidelines of the Italian Ministry of Health (Legislative Decree No. 26/2014) and European Union (Directive No. 2010/63/UE) legislations on animal research. All efforts were made to minimize the number of animals used and their suffering.

Electrode Implantation and tDCS Protocol

TDCS over the hippocampus was delivered using a unilateral epicranial electrode arrangement as previously described (Podda et al., 2016; Barbati et al., 2019). The active electrode consisted of a tubular plastic cannula (internal diameter 3.0 mm) filled with saline solution (0.9% NaCl) just prior to stimulation; the counter electrode was a conventional rubber-plate electrode surrounded by a wet sponge (5.2 cm²) positioned over the ventral thorax. The center of the active electrode was positioned on the skull over the left hippocampal formation 1 mm posterior and 1 mm lateral to the bregma (Franklin and Paxinos, 1997). A unilateral arrangement was chosen, as in our previous study, to reduce the electrode contact area and to prevent currents bypassing the two juxtaposed epicranial electrodes, which might occur using a bipolar configuration. Stimulation of the left side was preferred since experimental evidence suggests that long-term

memory processing are strictly dependent on this hemisphere (Shipton et al., 2014). This electrode montage was previously shown to target the hippocampus causing neurophysiological, behavioral and molecular changes all related to this brain structure. Furthermore, no changes in BDNF levels were detected in non-stimulated areas such as the cerebellum, and tDCS of the motor cortex caused no changes in the hippocampus (see details in Podda et al., 2016). For electrode implant, animals were anesthetized by an intraperitoneal injection of a cocktail with ketamine (87.5 mg/Kg) and xylazine (12.5 mg/Kg) and temperature during surgery was maintained at 37°C. The scalp and underlying tissues were removed and the electrode was implanted using a carboxylate cement (3M ESPE, Durelon, 3M Deutschland GmbH, Germany). All animals were allowed to recover for 3–5 days before tDCS. During this period, as well as during the electrical stimulations, mice were placed in individual cages.

TDCS was applied to awake mice using a battery-driven, constant current stimulator (BrainSTIM, EMS, Italy). The current intensity was ramped for 10 s instead of switching it on and off to avoid a stimulation break effect.

A repeated tDCS protocol was used consisting in 3 single stimulation sessions (at a current intensity of 250 μ A for 20 min, current density of 35.4 A/m²) once per day, on 3 consecutive days. According to clinical and brain slice conventions (Jackson et al., 2016; Rahman et al., 2017), we applied “anodal” tDCS corresponding to a positive electric field (positive electrode over the hippocampus). Electrode montage and current density were similar to those recently adopted for rodent models and close to the recommended safety limits in rodents (Rohan et al., 2015; Podda et al., 2016; Jackson et al., 2017; Paciello et al., 2018).

On the 3 consecutive days, tDCS was performed approximately at the same time (around 10 a.m.). No abnormal behaviors were observed related to the stimulation and no morphological alterations were found in brain tissues of mice subjected to tDCS.

Three-month-old WT and 3 \times Tg-AD mice were randomly assigned to the following experimental groups: (i) sham mice (sham-WT-3M, sham-3 \times Tg-AD-3M), which underwent the same manipulations as in the “real” stimulation condition, but no current was delivered; (ii) tDCS mice (tDCS-WT-3M, tDCS-3 \times Tg-AD-3M), which were subjected to repeated anodal tDCS. Different groups of mice were used for each experimental test.

Electrophysiology

Field recordings were performed on hippocampal coronal slices (400 μ m-thick) as previously described (Podda et al., 2008, 2016). Briefly mice were anesthetized by isoflurane inhalation (Esteve) and decapitated. The brain was rapidly removed and placed in ice-cold cutting solution (in mM: 124 NaCl, 3.2 KCl, 1 NaH₂PO₄, 26 NaHCO₃, 2 MgCl₂, 1 CaCl₂, 10 glucose, 2 sodium pyruvate, and 0.6 ascorbic acid, bubbled with 95% O₂-5% CO₂; pH 7.4). Slices were cut with a vibratome (VT1200S) and incubated in artificial cerebrospinal fluid (aCSF; in mM: 124 NaCl; 3.2 KCl; 1 NaH₂PO₄, 26 NaHCO₃, 1 MgCl₂, 2 CaCl₂, 10 glucose; 95% O₂-5% CO₂; pH 7.4) at 32°C for 60 min and then at RT until use. Slices were prepared ~30 min after tDCS or sham stimulation

protocol. Slices containing the stimulated hippocampus were used for subsequent analyses.

Slices were transferred to a submerged recording chamber and continuously perfused with aCSF (flow rate: 1.5 ml/min). The bath temperature was maintained at 30–32°C with an in-line solution heater and temperature controller (TC-344B, Warner Instruments). Identification of slice subfields and electrode positioning were performed with 4 \times and 40 \times water immersion objectives on an upright microscope (BX51WI, Olympus) and video observation (C3077-71 CCD camera, Hamamatsu Photonics).

All recordings were made using MultiClamp 700B amplifier (Molecular Devices). Data acquisition and stimulation protocols were performed with the Digidata 1440A Series interface and pClamp 10 software (Molecular Devices). Data were filtered at 1 kHz, digitized at 10 kHz, and analyzed both online and offline.

Field recordings were made using glass pipettes filled with aCSF (tip resistance 2–5 M Ω) and placed in the stratum radiatum of the CA1 region. Field excitatory post-synaptic potentials (fEPSPs) were evoked by stimulation of the Schaffer collateral using a concentric bipolar tungsten electrode (FHC) connected to a constant current isolated stimulator (Digitimer Ltd.). The stimulation intensity that produced one-third of the maximal response was used for the test pulses and LTP induction. The fEPSP amplitude was measured from baseline to peak. The slope of the rising phase of the fEPSP was also calculated.

For LTP recordings, stable baseline responses were recorded to test stimulations (0.05 Hz for 10 min) and then a high-frequency stimulation (HFS) protocol was delivered (4 trains of 50 stimuli at 100 Hz, 500 ms each, repeated every 20 s). Responses to test pulses were recorded every 20 s for 60 min to assess LTP. LTP was expressed as the percentage of change in the mean fEPSP slope or peak amplitude normalized to baseline values (i.e., mean values for the last 5 min of recording before HFS, taken as 100%). HFS-elicited fEPSP changes in both amplitude and slope higher than 15% of baseline values were subjected to data analysis.

Memory Test

Object recognition test, also known as novel object recognition (NOR) test and Morris water maze (MWM) test were used to assess non-spatial (i.e., recognition) and spatial memory, respectively. These tests were chosen since they are the most widely used and standardized tests of hippocampal-dependent forms of learning and memory (Vorhees and Williams, 2014; Cohen and Stackman, 2015).

Behavioral tests were carried out from 9 a.m. to 4 p.m. and data were blindly analyzed using an automated video tracking system (Any-Maze).

The NOR protocol lasted 3 consecutive days including a familiarization session, a training session and a test session. On the first day, animals were familiarized for 10 min to the test arena (45 cm \times 45 cm). On the second day (training session), they were allowed to explore two identical objects placed symmetrically in the arena for 10 min. On the third day (test session), a new object replaced one of the old objects. Animals were allowed to explore for 10 min and a preference index, calculated as the ratio between time spent exploring the novel object and time spent

exploring both objects, was used to measure recognition memory (Fusco et al., 2019).

MWM was performed as previously described (Podda et al., 2014, 2016). A circular plastic pool (127 cm in diameter) filled with water colored with nontoxic white paint, to obscure the location of an hidden platform, was used as experimental apparatus. The pool was ideally separated into four equal quadrants (NE, corresponding to the target quadrant, SE, NW, and SW) and the platform (10 cm × 10 cm) was placed at the center of the target quadrant. Visual cues were placed on the walls around the pool to orient the mice. Animals were trained for 4 days, six times a day and the probe test was administered 24 h after the last training day. Starting positions were varied daily and latencies to reach the platform were recorded. In the probe test, the platform was removed and time spent in the target quadrant was measured (60 s of test duration).

According to published protocols, the following exclusion criteria were applied: total exploration time < 5 s in the NOR test and floating behavior during training (i.e., not actively searching for the platform) in the MWM test. No animal met exclusion criteria and all results of behavioral studies were included in data analysis.

Western Immunoblot

Total proteins were extracted from the stimulated hippocampus of control and tDCS-mice sacrificed 2 h after stimulation, using ice cold RIPA buffer [Pierce; 50 mM Tris, 150 mM NaCl, 1 mM EDTA, 1% DOC, 1% Triton X-100, 1% SDS, and 1 × protease, phosphatase-1, and phosphatase-2 inhibitor cocktails (Sigma)]. Tissues were incubated for 15 min on ice with occasional vortexing and the lysate was spun down at 22,000 × g for 15 min, 4°C, and 2 μl aliquot of the supernatant was assayed to determine the protein concentration (microBCA kit, Pierce). SDS-PAGE reducing sample buffer was added to the supernatant, and samples were heated to 95°C for 5 min. Protein lysates (40 μg) were loaded onto 10% or 8% Tris-glycine polyacrylamide gels for electrophoretic separation. Precision Plus Protein Dual Color Standards (Bio-Rad) were used as molecular mass standards. Proteins were then transferred onto nitrocellulose membranes at 330 mA for 2 h at 4°C in transfer buffer containing 25 mM Tris, 192 mM glycine and 20% methanol. Membranes were incubated for 1 h with blocking buffer (5% skim milk in TBST), and then incubated overnight at 4°C with primary antibodies directed against one of the following proteins: pCREB^{Ser133}, CREB, pCaMKII^{Thr286}, CaMKII, and GAPDH (Supplementary Table 1). After three 10 min rinses in TBST, membranes were incubated for 2 h at RT with HRP-conjugated secondary antibodies (Supplementary Table 1). The membranes were then washed, and the bands were visualized with an enhanced chemiluminescence detection kit (GE Healthcare, United Kingdom). Protein expression was evaluated and documented using UVitec Cambridge Alliance. Experiments were performed in triplicate.

ELISA Measurements

Blood samples were collected from the retro-orbital plexus with sterile glass Pasteur pipettes. Samples were taken before

and 1 week after tDCS. After centrifugation, plasma was separated and stored at −80°C until further use. Plasma levels of BDNF were determined using commercially available ELISA kits (Immunological Sciences). The assay was performed according to the manufacturer's instructions on samples collected from 4 animals per group, and each sample was analyzed in duplicate.

Statistical Analysis

Sample sizes were chosen with adequate statistical power (0.8) according to results of prior pilot data sets or studies, including our own using similar methods or paradigms. Sample estimation and statistical analysis were performed using the SigmaPlot 14.0 software. Data were first tested for equal variance and normality (Shapiro-Wilk test) and then the appropriate statistical tests were chosen. The statistical tests used [i.e., one-way ANOVA, one-way ANOVA for repeated measures (RM), Friedman RM ANOVA on Ranks, two-way ANOVA, two-way RM ANOVA] are indicated in the main text and in the corresponding figure legends for each experiment. *Post hoc* multiple comparisons were performed with Bonferroni correction. The level of significance was set at 0.05. Results are presented as mean ± SEM. Analyses were performed blinded.

RESULTS

Characterization of Memory and Synaptic Plasticity Impairments in 3 × Tg-AD Mice

The objective of the study was to test whether anodal tDCS can be exploited to unmask covert impairment of brain plasticity mechanisms in 3 × Tg-AD mice before synaptic plasticity and memory deficits are clearly manifested in this AD mouse model, with the ultimate goal to identify early neurophysiological and molecular biomarkers allowing to predict disease onset.

Our first step was to characterize the time course of the 3 × Tg-AD mouse phenotype in our experimental conditions, given that some variability has been reported in literature (Belfiore et al., 2019). Specifically, memory and LTP were assessed in 3 and 7 months old AD mice, chosen as putative pre-symptomatic and AD models, respectively. Different cohorts of mice were used for 3 and 7 months.

Results were compared to those obtained in age-matched WT animals. We found that, at 3 months of age, 3 × Tg-AD mice did not exhibit any impairment in recognition and spatial memory, as assessed by NOR and MWM tests, respectively (Figures 1A–C). In particular, in the NOR test the preference index was comparable in 3 × Tg-AD and age-matched WT mice (63.8 ± 1.7% and 65.7 ± 1.7%, respectively, $n = 9$ for each group; $P = 0.40$, one-way ANOVA; Figure 1A; exploration time: WT-3M mice, novel object (NO) 11.3 ± 1 s, familiar object (FO) 5.9 ± 0.5 s; 3 × Tg-AD-3M mice, NO 11.5 ± 2.6 s, FO 6.4 ± 1.3 s). Similarly, in the acquisition session of the MWM, all mice successfully acquired the task with latency to reach the platform decreasing progressively across training days [main effect of days: $F_{(3, 48)} = 34.13$, $P < 0.001$, two-way RM ANOVA] and no

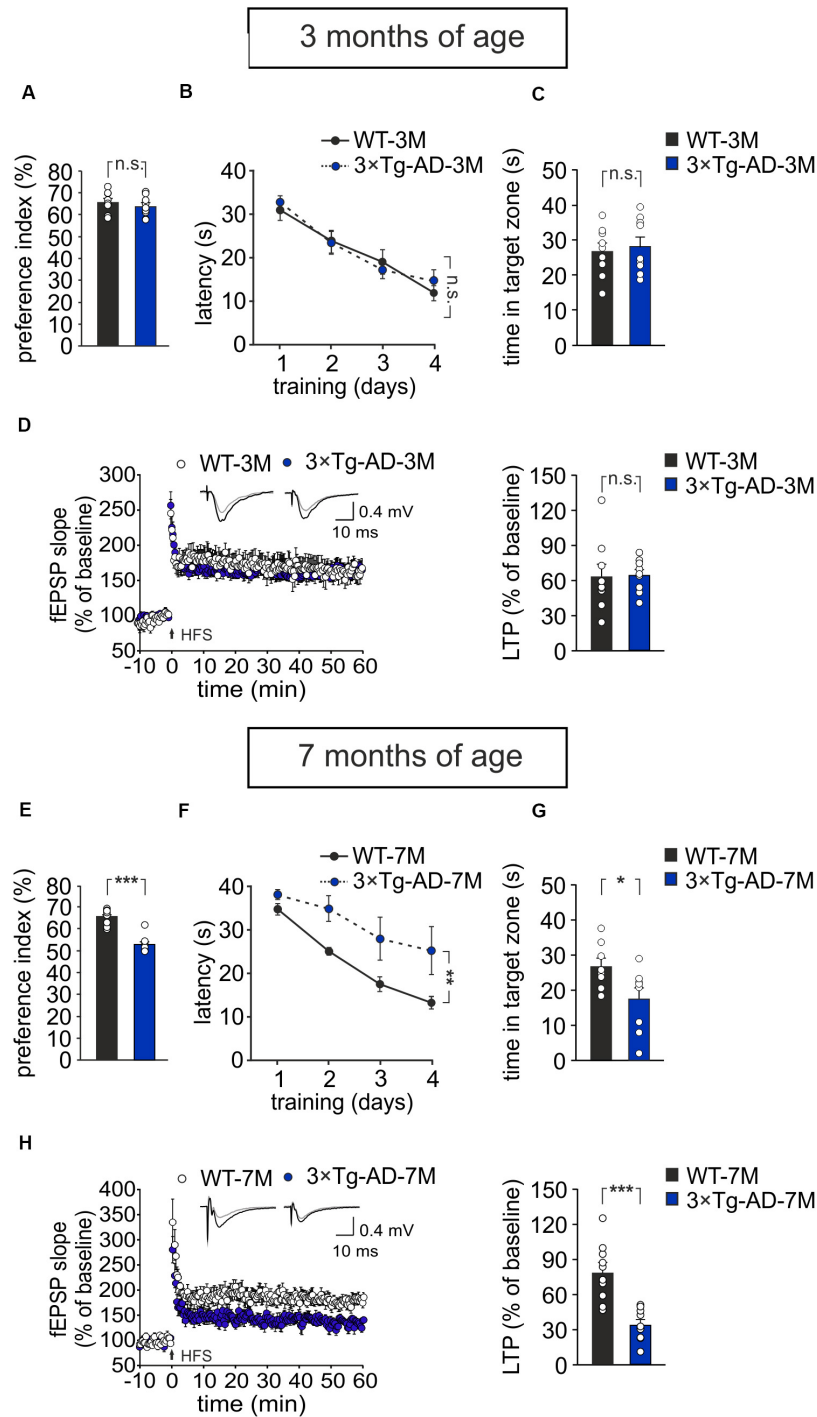


FIGURE 1 | Age-dependent pathological memory and synaptic plasticity changes in 3 × Tg-AD mice. **(A–D)** 3-month-old 3 × Tg-AD mice did not differ from age-matched WT mice in: **(A)** the preference toward the novel object in the NOR test ($n = 9$ mice for each group; $P = 0.40$, one-way ANOVA); **(B)** the latency to platform in the training phase of the MWM ($n = 9$ mice for each group; $P = 0.73$, two-way RM ANOVA) and **(C)** the time spent in the target quadrant during the probe test performed on day 5 of MWM ($P = 0.66$, one-way ANOVA); **(D)** the magnitude of LTP at hippocampal CA3-CA1 synapses ($n = 9$ slices from 5 3 × Tg-AD-3M mice; $n = 9$ slices from 6 WT-3M mice; $P = 0.89$, one-way ANOVA). Time course shows LTP at CA3-CA1 synapses induced by HFS (4 trains of 50 stimuli at 100 Hz for 500 ms repeated every 20 s) delivered at time 0 (arrow). Results are expressed as percentages of baseline fEPSP slope (= 100%). Insets show representative fEPSPs at baseline (gray line) and during the last 5 min of LTP recording (black line). Bar graphs compare LTP observed during the last 5 min of recording. **(E–H)** Compared to aged-matched WT mice, 7-month-old 3 × Tg-AD mice showed significant decreases in: **(E)** preference index in the NOR test ($P < 0.001$); **(F)** latency to platform in the training phase of the MWM test ($n = 8$ mice for each group $P = 0.009$, two-way RM ANOVA) and **(G)** time spent in the target quadrant during the probe test of MWM ($P = 0.032$, one-way ANOVA); **(H)** LTP ($n = 10$ slices from 5 3 × Tg-AD-7M mice; $n = 10$ slices from 5 WT-7M mice, $P = 0.0001$, one-way ANOVA). Data are expressed as mean ± SEM. * $P < 0.05$; ** $P < 0.01$; *** $P < 0.001$; n.s., not significant.

571 significant differences between WT-3M and 3 × Tg-AD-3M mice
 572 in all trials ($n = 9$ for each group; $P = 0.73$, two-way RM ANOVA;
 573 **Figure 1B**) were noted. In the probe test, the time spent in
 574 the target quadrant was similar in 3 × Tg-AD-3M and WT-
 575 3M mice (28.6 ± 2.8 s vs. 27.0 ± 2.5 s, respectively, $P = 0.66$,
 576 one-way ANOVA; **Figure 1C**). Both groups spent significantly
 577 more time in the target quadrant compared to random quadrant
 578 occupancy [i.e., 15 s; WT-3M mice, $F_{(1, 19)} = 16.38$, $P = 0.0006$;
 579 3 × Tg-AD-3M mice, $F_{(1, 19)} = 18.50$, $P = 0.0003$, one-way
 580 ANOVA]. Memory deficits were, instead, manifested in 7-month-
 581 old 3 × Tg-AD mice (3 × Tg-AD-7M). In the NOR test, they
 582 showed a lower preference index than age-matched WT mice
 583 ($53.2 \pm 1.5\%$ vs. $65.6 \pm 1.4\%$ in WT-7M mice; $n = 8$ for each
 584 group; $P < 0.001$, one-way ANOVA; **Figure 1E**; exploration time:
 585 WT-7M mice, NO 9.2 ± 1.2 s, FO 4.9 ± 0.7 s; 3 × Tg-AD-7M,
 586 NO 6.2 ± 1.5 s, FO 5.5 ± 1.3 s). In the acquisition session of the
 587 MWM, all mice displayed decreased latency to reach the hidden
 588 platform over training days [main effect of days: $F_{(3, 42)} = 14.72$,
 589 $P < 0.001$, two-way RM ANOVA, but 3 × Tg-AD-7M mice took
 590 longer time to find the platform than WT-7M mice ($n = 8$ for
 591 each group; $P = 0.009$, two-way RM ANOVA; **Figure 1F**). In the
 592 probe test, 3 × Tg-AD-7M mice explored the target quadrant
 593 less than controls (17.4 ± 3.5 s vs. 27.0 ± 2.5 s in WT-7M mice;
 594 $P = 0.032$, one-way ANOVA; **Figure 1G**). Finally, WT-7M mice
 595 spent significantly more time in the target quadrant compared to
 596 random quadrant occupancy while 3 × Tg-AD-7M mice failed to
 597 do so [WT-7M mice, $F_{(1, 18)} = 16.17$, $P = 0.0008$; 3 × Tg-AD-7M
 598 mice, $F_{(1, 18)} = 0.85$, $P = 0.36$, one-way ANOVA].

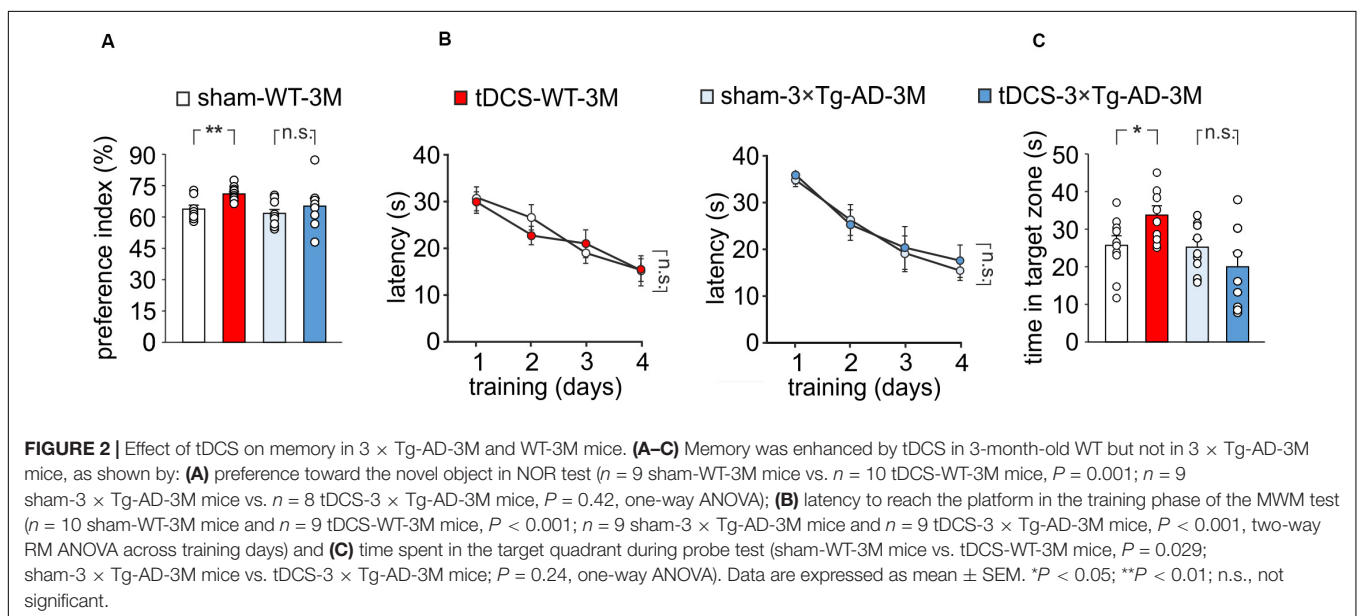
599 As expected, behavioral data were paralleled by
 600 electrophysiological data showing a significant reduction of
 601 LTP at CA3–CA1 hippocampal synapses in brain slices from
 602 3 × Tg-AD-7M mice [$34.37 \pm 4.36\%$; ($n = 10$ slices from 5 mice)
 603 vs. $78.85 \pm 8.09\%$ ($n = 10$ slices obtained from 5 WT-7M mice);
 604 $P = 0.0001$, one-way ANOVA; **Figure 1H**], whereas LTP was not
 605 significantly different in transgenic and WT mice at 3 months of

628 age [$65.11 \pm 4.86\%$ ($n = 9$ slices from 5 3 × Tg-AD-3M mice) vs.
 629 $63.68 \pm 10.74\%$ ($n = 9$ slices from 6 WT-3M mice); $P = 0.89$,
 630 one-way ANOVA; **Figure 1D**]. Data reported above refer to
 631 analysis of fEPSP slope. A similar picture emerged when LTP
 632 was assessed by analyzing fEPSP amplitude (**Supplementary**
 633 **Figures 1A,B**). In agreement with our previous result (Leone
 634 et al., 2019) Western immunoblot experiments, performed with
 635 the 6E10 antibody recognizing human A β , revealed A β oligomers
 636 in hippocampal lysates of 3 × Tg-AD-7M mice (**Supplementary**
 637 **Figure 1C**). A faint band was observed at the same molecular
 638 weight in tissues from 3 × Tg-AD-3M.

639 Altogether these data indicate that, at 3 months of age, 3 × Tg-
 640 AD mice do not show synaptic plasticity and memory deficits
 641 and, therefore, they are a suitable model of a pre-symptomatic
 642 AD stage to test our hypothesis.

644 Anodal tDCS Fails to Enhance 645 Recognition and Spatial Memory in 646 3 × Tg-AD-3M Mice

647 We then compared memory performances of 3 × Tg-AD-3M
 648 and age-matched WT mice subjected to a protocol of triple tDCS
 649 or sham stimulation. Consistently with our previous findings
 650 (Podda et al., 2016), WT mice subjected to tDCS showed a
 651 greater preference toward the novel object than sham-stimulated
 652 mice [preference index: $70.7 \pm 1.1\%$ ($n = 10$) and $63.5 \pm 1.8\%$
 653 ($n = 9$), respectively, $P = 0.001$, one-way ANOVA; **Figure 2A**].
 654 As expected from data reported above, sham-3 × Tg-AD-
 655 3M mice showed intact recognition memory [preference index:
 656 $61.0 \pm 2.1\%$ ($n = 9$), $P = 0.36$ vs. sham-WT-3M mice, one-
 657 way ANOVA; **Figure 2A**]. Of note, preference for the novel
 658 object was not increased by tDCS in 3 × Tg-AD-3M mice
 659 [preference index: $64.6 \pm 4.3\%$ ($n = 8$), $P = 0.42$ vs. sham-3 × Tg-
 660 AD-3M mice, ($n = 9$) one-way ANOVA; **Figure 2A**]. Similar
 661 results were obtained with MWM, as shown in **Figures 2B,C**.



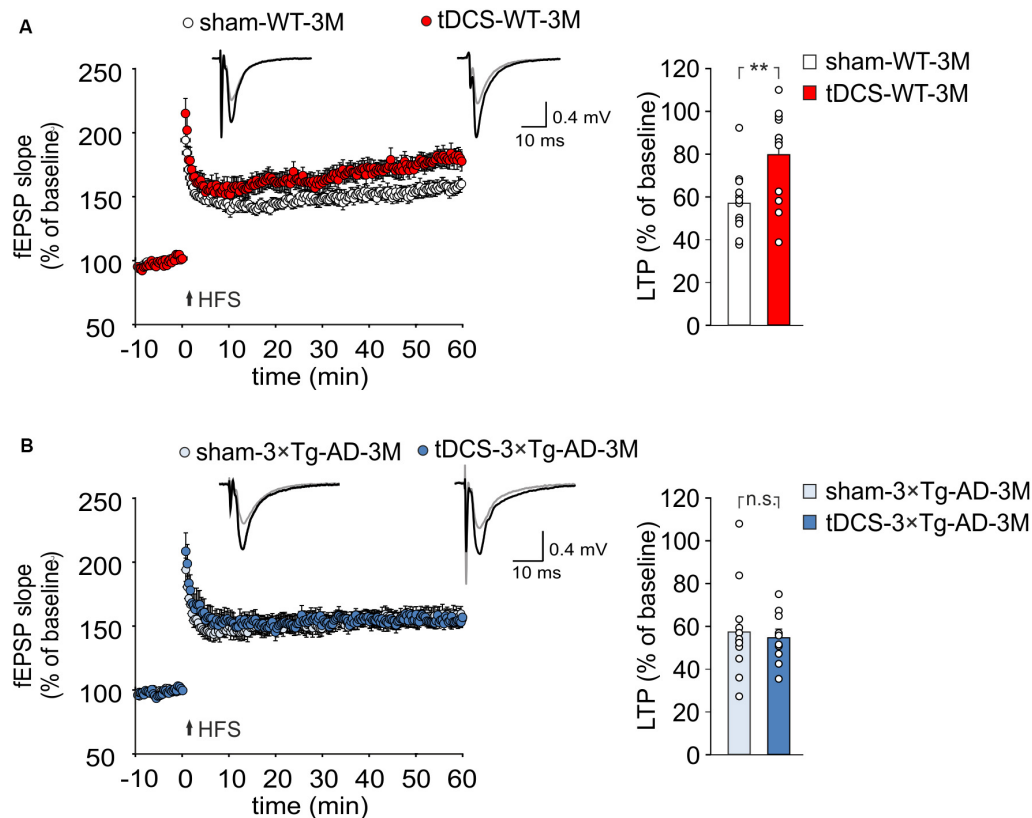


FIGURE 3 | tDCS differentially impacts hippocampal LTP in 3 × Tg-AD-3M and WT mice. **(A,B)** Time course of LTP at CA3-CA1 synapses induced by HFS delivered at time 0 (arrow). Results are expressed as percentages of baseline fEPSP slope (= 100%). Insets show representative fEPSPs at baseline (gray line) and during the last 5 min of LTP recording (black line). Bar graphs compare LTP observed during the last 5 min of recording. **(A)** Slices obtained from tDCS-WT-3M mice ($n = 12$ slices from 7 mice) showed enhanced LTP compared to sham-WT-3M mice ($n = 12$ slices from 9 mice, $P = 0.007$, one-way ANOVA). **(B)** tDCS failed to enhance LTP in 3 × Tg-AD-3M mice ($n = 10$ slices from 5 tDCS mice; $n = 12$ slices from 5 sham mice, $P = 0.71$; one-way ANOVA). Data are expressed as mean ± SEM; * $P < 0.05$; n.s., not significant.

In the acquisition session of the MWM, all mice successfully acquired the task with latency to reach the platform decreasing progressively across training days [WT-3M mice: main effect of days: $F_{(3, 51)} = 23.85$, $P < 0.001$, two-way RM ANOVA; 3 × Tg-AD-3M mice: main effect of days: $F_{(3, 48)} = 21.33$, $P < 0.001$, two-way RM ANOVA; **Figure 2B**], with no significant differences between sham and tDCS in both groups (WT-3M mice: $P = 0.81$; 3 × Tg-AD-3M: $P = 0.71$, two-way RM ANOVA). In the probe test, WT mice, but not 3 × Tg-AD-3M mice, showed improvement following tDCS [tDCS-WT-3M, 33.5 ± 2.5 s ($n = 9$) vs. 25.5 ± 2.5 s ($n = 10$) sham-WT-3M; $P = 0.029$, one-way ANOVA; tDCS-3 × Tg-AD-3M, 19.8 ± 3.9 s ($n = 9$) vs. 24.9 ± 2.2 s ($n = 9$) sham-3 × Tg-AD-3M; $P = 0.24$, one-way ANOVA; **Figure 2C**].

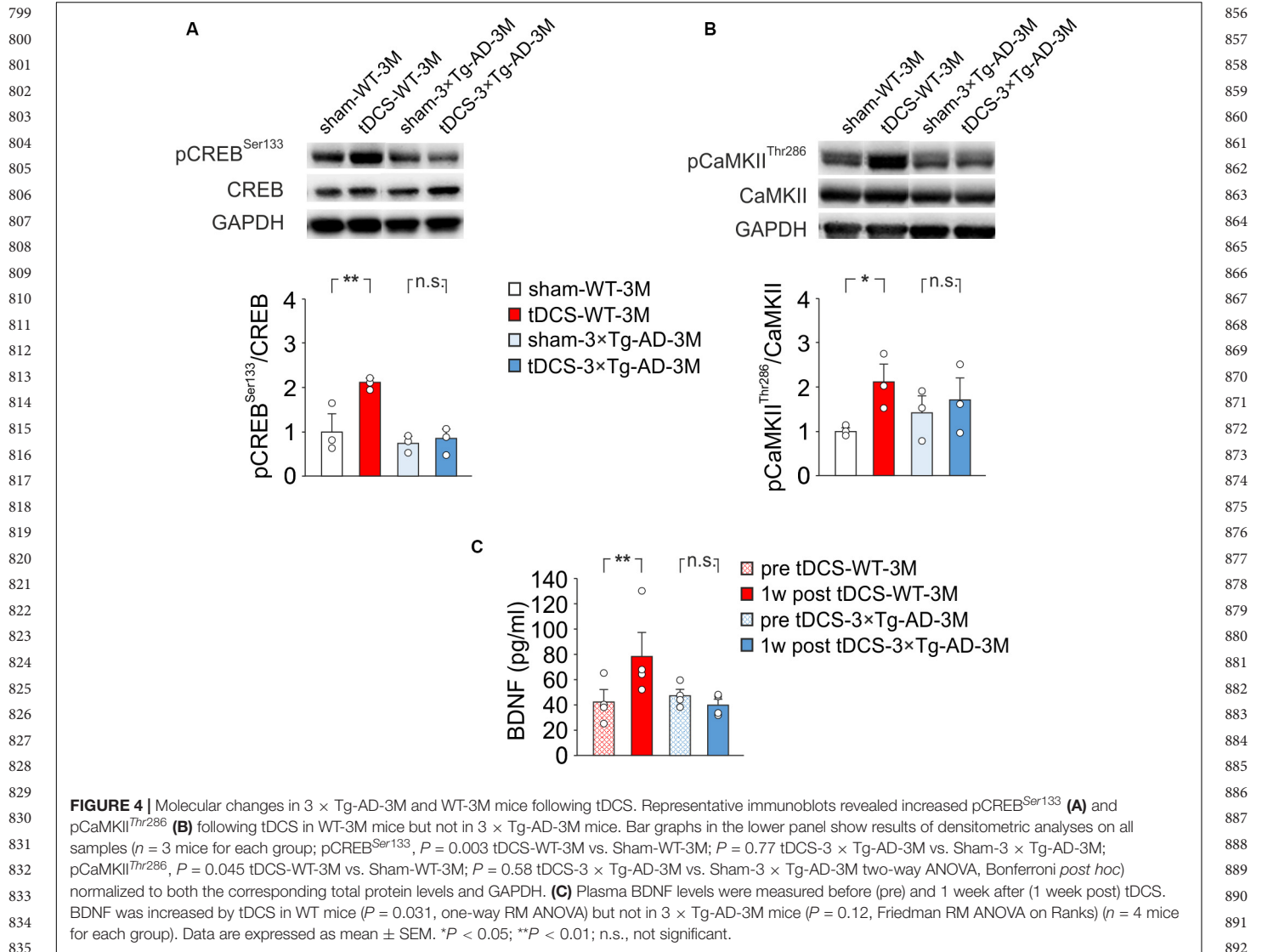
Anodal tDCS Fails to Enhance LTP in 3 × Tg-AD-3M Mice

TDCS effects on memory have been reportedly associated to increased hippocampal LTP (Podda et al., 2016; Yu et al., 2019). We therefore asked whether the behavioral unresponsiveness to tDCS of 3 × Tg-AD-3M mice was associated to the lack of tDCS

effects on synaptic plasticity. FEPSP slope was measured in the CA1 area after standard HFS of Schaffer collaterals and LTP was studied in slices from WT and 3 × Tg-AD-3M mice subjected to tDCS or sham stimulation. Sixty min after HFS, slices from tDCS-WT mice showed significantly greater LTP than slices from sham-WT mice [$79.65 \pm 6.58\%$ ($n = 12$ slices from 7 tDCS mice) vs. $57.0 \pm 4.4\%$ ($n = 12$ slices from 9 sham mice); $P = 0.007$, one-way ANOVA; **Figure 3A** and **Supplementary Figure 2A**]. Conversely, LTP was not increased by tDCS in 3 × Tg-AD-3M mice [$54.71 \pm 3.89\%$ ($n = 10$ slices from 5 tDCS mice) vs. $57.49 \pm 6.23\%$ ($n = 12$ slices from 5 sham mice); $P = 0.71$, one-way ANOVA; **Figure 3B** and **Supplementary Figure 2B**], demonstrating that in these mice the cellular correlate of memory is also resistant to the boosting action of tDCS.

Molecular Determinants of Plasticity Are Resistant to tDCS Boosting Effects in 3 × Tg-AD-3M Mice

The above reported results demonstrate that, before the AD-like phenotype is manifested, 3 × Tg-AD mice – despite normal memory and hippocampal LTP – exhibit decreased



responsiveness to the boosting action of tDCS. The reduced response to tDCS might result from initial dysfunction of the molecular pathways underlying plasticity that are challenged by tDCS.

To test this hypothesis, we performed molecular analyses on hippocampi and blood samples from WT and 3 × Tg-AD-3M mice subjected to tDCS or sham stimulation. Our analyses were focused on known upstream mechanisms of tDCS action, such as Ca²⁺-dependent phosphorylation of CREB at Ser133 and of CaMKII at Thr286, and a pivotal downstream effector, i.e., the neurotrophin BDNF (Podda et al., 2016; Kim et al., 2017; Paciello et al., 2018; Stafford et al., 2018; Barbati et al., 2019).

Our previous observations indicated that tDCS induced CREB activation in the hippocampus 2 h after stimulation (Podda et al., 2016). Accordingly, immunoblot analyses revealed that, 2 h after the end of the last tDCS session, hippocampi of WT mice ($n = 3$) showed increased levels of pCREB^{Ser133} [+110% vs. sham-WT-3M mice ($n = 3$), $P = 0.003$; two-way ANOVA, Bonferroni

post hoc; Figure 4A] and pCaMKII^{Thr286} (+109% vs. sham-WT-3M mice, $P = 0.045$ two-way ANOVA, Bonferroni *post hoc*; Figure 4B). Intriguingly, these post-translational modifications were not observed in 3 × Tg-AD-3M mice following tDCS (pCREB^{Ser133}: +11% vs. sham-3 × Tg-AD-3M mice; $P = 0.77$; pCaMKII^{Thr286}: +19% vs. sham-3 × Tg-AD-3M mice; $P = 0.58$; two-way ANOVA, Bonferroni *post hoc*; $n = 3$ mice each group; Figures 4A,B).

We previously reported that enhanced pCREB^{Ser133} following tDCS increases BDNF expression in the hippocampus by epigenetic regulation of *Bdnf* promoter I (Podda et al., 2016), and similar results were observed in auditory and motor cortices exposed to tDCS (Paciello et al., 2018; Barbati et al., 2019). We, therefore, hypothesized that tDCS could differentially impact BDNF expression in WT-3M and 3 × Tg-AD-3M mice. Given that changes of brain BDNF expression are reflected in blood (Laske et al., 2006; Brunoni et al., 2015), we asked whether assessment of changes in plasma BDNF following tDCS could

be a reliable biomarker of altered brain plasticity in AD. Blood samples used for BDNF testing were collected from each studied mice before starting the tDCS and 1 week after the completion of the tDCS protocol. This time point was chosen based on the results of a meta-analysis showing that increased plasma BDNF levels are more frequently observed some days after different protocols of non-invasive brain stimulation (NIBS) than soon after (Brunoni et al., 2015), and our previous studies demonstrated enhanced BDNF expression in the hippocampus 1 week after tDCS (Podda et al., 2016).

Remarkably, we found that plasma BDNF levels were significantly increased after tDCS in WT-3M (78.5 ± 20.2 vs. 42.3 ± 9.9 pg/ml pre-stimulation; $n = 4$ mice, $P = 0.031$, one-way RM ANOVA) but not in $3 \times$ Tg-AD-3M mice (40.1 ± 4.9 vs. 47.8 ± 5.0 pg/ml pre-stimulation; $n = 4$ mice, $P = 0.12$, Friedman RM ANOVA on Ranks; **Figure 4C**).

Our findings indicate that in $3 \times$ Tg-AD-3M mice molecular determinants of plasticity such as CREB, CaMKII and BDNF are resistant to the boosting effects of tDCS. More importantly, the early impairment of molecular machinery underlying synaptic plasticity and memory in $3 \times$ Tg-AD-3M mice can be detected by BDNF blood testing following tDCS.

DISCUSSION

AD is the most common form of dementia in elderly, characterized by a severe and progressive cognitive decline. So far, no effective treatments have been identified, but accumulating evidence suggests that therapeutics might work best if started at an early disease stage. The preclinical and prodromal phases of AD are considered promising time-windows for disease-modifying interventions (Galluzzi et al., 2016; Joe and Ringman, 2019). Therefore, early diagnosis is critical to successfully implement effective treatments.

The diagnosis of preclinical and prodromal AD is presently performed using cerebrospinal fluid analysis, neuroimaging investigations and neuropsychological testing (Lashley et al., 2018). Recently, graph theory analysis of brain connectivity from EEG signals combined with apolipoprotein E genotyping has been proposed to distinguish prodromal to AD from non-prodromal mild cognitive impairment (MCI) subjects (Vecchio et al., 2018). While these diagnostic approaches are valid and reliable, they cannot be employed for a wide ranging screening of persons at risk of AD, because they are invasive, expensive and require equipment and expertise usually only available in specialized hospitals.

Looking for an easy, non-invasive, low-cost and affordable method to screen populations at risk of AD, we investigated brain plasticity responses to tDCS in an AD mouse model before phenotype manifestation. This approach unveiled early electrophysiological and molecular dysfunction leading to the unresponsiveness of $3 \times$ Tg-AD-3M mice to tDCS boosting effects on memory, LTP and molecular determinants of synaptic plasticity.

Our data suggest that the assessment of plasticity-related molecular biomarkers before and after tDCS could represent

a novel approach to predict AD onset and progression. Of particular relevance for a translational point of view, are the differential effects of tDCS on plasma BDNF levels.

In this study 3-month-old $3 \times$ Tg-AD mice were used as a model of preclinical AD. These mice showed normal memory, as their performance in the NOR and MWM tests was similar to that of age-matched WT mice. At 3 months of age LTP values were also comparable in WT and transgenic mice. Impaired memory and LTP were, instead, observed in AD mice at 7 months of age. Although a certain degree of $3 \times$ Tg-AD mouse model heterogeneity has been reported regarding the onset and progression of cognitive deficits, the timeline of the AD phenotype, in our experimental conditions, is in agreement with literature (Chakroborty et al., 2019; Joseph et al., 2019).

The NIBS techniques have recently gained considerable attention as promising approaches to slow the progression of AD (Rajji, 2019a). Despite encouraging data, conflicting results have been reported so far, likely due to different study designs, patient selection criteria, populations, or sample sizes, therefore, the efficacy of NIBS in AD is still uncertain (Rajji, 2019b). As far as animal models are concerned, tDCS failed to rescue learning and memory deficits in $3 \times$ Tg-AD mice when the phenotype is manifested (i.e., >6 months of age) (Gondard et al., 2019).

We propose to use tDCS in AD differently, namely, as a tool to probe and challenge plasticity pathways in the pre-symptomatic phase of the disease in order to unveil their earliest alterations.

Indeed, several studies, including our own, indicated that molecular determinants of plasticity and, particularly, the neurotrophin BDNF, are engaged and boosted by anodal tDCS, leading to enhanced plasticity and memory (Rohan et al., 2015; Podda et al., 2016; Kim et al., 2017; Cocco et al., 2018; Paciello et al., 2018; Stafford et al., 2018; Barbati et al., 2019; Kronberg et al., 2020).

Consistently, we found that 3-month-old WT mice, subjected to a daily session of anodal tDCS for three consecutive days, showed enhanced hippocampus-dependent recognition and spatial memory as assessed by NOR and MWM tests as well as enhanced LTP – the cellular underpinning of memory (Bliss and Collingridge, 1993). Interestingly enough, none of these effects was seen in $3 \times$ Tg-AD-3M mice.

We, therefore reasoned that the lack of tDCS effects on LTP and memory in $3 \times$ Tg-AD-3M mice might be due to the unsuccessful recruitment of plasticity-related pathways. We previously identified the signaling cascade engaged by tDCS in the hippocampus, including increased CREB phosphorylation at Ser133 that triggers epigenetic modifications relying on CREB binding to the *Bdnf* promoter I and recruitment of the histone acetyltransferase CREB-binding protein leading to enhanced acetylation at lysine 9 on *Bdnf* promoter I and increased BDNF expression. Blockade of H3 acetylation as well as of BDNF-specific TrkB receptors hindered tDCS effects on LTP and memory. Collectively, data summarized above suggested a causal link among the tDCS-induced increases in: (i) CREB phosphorylation; (ii) BDNF expression; (iii) synaptic plasticity; and (iv) memory (Podda et al., 2016). It has also been hypothesized that molecular events underlying tDCS effects are initiated by increased Ca^{2+} signaling via

1027 NMDAR and voltage-gated calcium channel activation (Pelletier
1028 and Cicchetti, 2014; Rohan et al., 2015). Indeed, Ca^{2+} -
1029 dependent intracellular responses observed following tDCS
1030 include increased phosphorylation of CREB and CaMKII along
1031 with nitric oxide synthase activation (Kim et al., 2017; Cocco
1032 et al., 2018; Barbati et al., 2019). In keeping with these data, our
1033 Western immunoblot analyses showed enhanced pCREB^{Ser133}
1034 and pCaMKII^{Thr286} in tDCS-WT-3M mice. Of relevance, the
1035 lack of tDCS effects on LTP and memory in $3 \times$ Tg-AD-3M
1036 mice was paralleled by its inability to enhance pCREB^{Ser133}
1037 and pCaMKII^{Thr286}, indicating that these differential response
1038 could serve as novel AD biomarker. Investigating the role
1039 of Ca^{2+} signal dysregulation in the tDCS ineffectiveness on
1040 LTP and memory in $3 \times$ Tg-AD-3M mice was beyond the
1041 scope of this research. However it is worth mentioning that
1042 enhanced Ca^{2+} signaling has been reported in the earliest stages
1043 of the disease in mouse AD models (Del Prete et al., 2014;
1044 Chakroborty et al., 2019) and it has also been observed in cells
1045 from familial AD patients (Nelson et al., 2010). Furthermore,
1046 convergent evidence indicates Ca^{2+} dyshomeostasis within
1047 synaptic compartments as an early and critical factor in driving
1048 synaptic pathophysiology, leading to cognitive impairment in AD
1049 (Whitcomb et al., 2015).

1050 The main purpose of our study was to identify an early
1051 and easy-to-detect AD biomarker potentially translatable to
1052 clinical application. Of course, molecular changes only occurring
1053 in the brain would not meet these requirements; therefore,
1054 we looked for biomarkers available in the circulating blood.
1055 Changes in pCREB and pCaMKII levels in the brain might
1056 be paralleled by similar changes in neuron-derived exosomes
1057 isolated from circulating blood, which is a promising though
1058 still experimental approach (Shi et al., 2016; Badhwar and
1059 Haqqani, 2020) we are planning to implement in future
1060 studies. Instead, we focused on a much simpler and cheaper
1061 approach, based on plasma BDNF level assessment by ELISA
1062 (Naegelin et al., 2018), which could be employed in any
1063 laboratory performing blood sample testing and therefore, widely
1064 accessible to any population. As already mentioned, enhanced
1065 BDNF expression in hippocampal lysates was demonstrated
1066 in our previous study following tDCS. Although different
1067 organs may contribute to determine plasma BDNF levels,
1068 several evidences suggest that changes in blood BDNF levels
1069 may reflect changes occurring in the brain. Indeed, changes
1070 in blood BDNF levels have been associated with a number
1071 of neurological diseases including AD (Laske et al., 2006),
1072 and they have also been more frequently reported days or
1073 weeks after stimulation following tDCS in different clinical
1074 conditions or experimental models (Brunoni et al., 2015).
1075 We, therefore, compared plasma BDNF levels before and
1076 1 week after tDCS and found that they were significantly
1077 increased in WT but not in $3 \times$ Tg-AD-3M mice. Investigating
1078 the specific contribution of hippocampus vs. other cortical
1079 and subcortical areas underneath the stimulating electrode
1080 to plasma BDNF levels as well as its different forms (i.e.,
1081 mature vs. pro-BDNF) was beyond the scope of this paper.
1082 Similarly, our study did not address the role of BDNF in AD
1083 pathophysiology.

1084 Instead, our novel finding provides a peripheral biomarker
1085 of covert neuroplasticity impairment that could be detected in
1086 blood samples and easily translated to clinical use. The non-
1087 invasiveness and lack of adverse effects of tDCS (Antal et al.,
1088 2017) support future longitudinal studies in patient cohorts at
1089 risk of AD including elderly people diagnosed for amnesic
1090 MCI or those with genetic risk factors. In summary, our study
1091 unravels the unresponsiveness of neuroplasticity mechanisms
1092 in the hippocampus to boost stimuli in a pre-AD stage. The
1093 combined use of a non-invasive method such as tDCS and plasma
1094 BDNF level assessment before and after treatment appears a
1095 novel promising approach to detect synaptic dysfunction far
1096 earlier than the appearance of any clinical signs. Although our
1097 findings still need to be validated in humans, they indicate a very
1098 promising perspective for large population analyses of subjects
1099 at risk to develop AD, with far reaching implications for both a
1100 personalized approach to AD patients and public health.

1103 DATA AVAILABILITY STATEMENT

1104 The raw data supporting the conclusions of this article will be
1105 made available by the authors, without undue reservation, to any
1106 qualified researcher. Q9

1110 ETHICS STATEMENT

1111 The animal study was reviewed and approved by the
1112 Ethics Committee of the Catholic University and Italian
1113 Ministry of Health. Q10

1117 AUTHOR CONTRIBUTIONS

1118 CG and MP conceived the study and supervised the work. SC, VL,
1119 PR, and GA performed the electrophysiological experiments. MR
1120 and AM performed the behavioral experiments. SF performed the
1121 ELISA experiments. KG and SF performed the WB experiments.
1122 DL performed the analysis of A β oligomers. MP and CG wrote
1123 the manuscript. All authors contributed to the article and
1124 approved the submitted version. Q11
Q12

1127 FUNDING

1128 This work was supported by the Italian Ministry of Health –
1129 Ricerca Finalizzata # RF-2013-02356444. Q13

1133 SUPPLEMENTARY MATERIAL

1134 The Supplementary Material for this article can be found online
1135 at: [https://www.frontiersin.org/articles/10.3389/fcell.2020.00541/
1136 full#supplementary-material](https://www.frontiersin.org/articles/10.3389/fcell.2020.00541/full#supplementary-material) Q14

REFERENCES

- 1141 Antal, A., Alekseichuk, I., Bikson, M., Brockmüller, J., Brunoni, A. R., and Chen,
1142 R. (2017). Low intensity transcranial electric stimulation: safety, ethical, legal
1143 regulatory and application guidelines. *Clin. Neurophysiol.* 128, 1774–1809. doi:
1144 10.1016/j.clinph.2017.06.001 1200
- 1145 Badhwar, A., and Haqqani, A. S. (2020). Biomarker potential of brain-secreted
1146 extracellular vesicles in blood in Alzheimer's disease. *Alzheimers Dement.*
1147 12:e12001. doi: 10.1002/dad2.12001 1204
- 1148 Barbati, S. A., Cocco, S., Longo, V., Spinelli, M., Gironi, K., Mattera, A., et al.
1149 (2019). Enhancing plasticity mechanisms in the mouse motor cortex by
1150 anodal transcranial direct-current stimulation: the contribution of nitric oxide
1151 signaling. *Cereb. Cortex* 30, 2972–2985. doi: 10.1093/cercor/bhz288 1205
- 1152 Bature, F., Guinn, B. A., Pang, D., and Pappas, Y. (2017). Signs and symptoms
1153 preceding the diagnosis of Alzheimer's disease: a systematic scoping review of
1154 literature from 1937 to 2016. *BMJ Open* 7:e015746. doi: 10.1136/bmjopen-2016-
1155 015746 1206
- 1155 Belfiore, R., Rodin, A., Ferreira, E., Velazquez, R., Branca, C., Caccamo, A.,
1156 et al. (2019). Temporal and regional progression of Alzheimer's disease-like
1157 pathology in 3xTg-AD mice. *Aging Cell* 18:e12873. doi: 10.1111/accel.12873 1207
- 1158 Bliss, T. V., and Collingridge, G. L. (1993). A synaptic model of memory: long-term
1159 potentiation in the hippocampus. *Nature* 361, 31–39. doi: 10.1038/361031a0 1208
- 1160 Bloom, G. S. (2014). Amyloid- β and tau: the trigger and bullet in Alzheimer disease
1161 pathogenesis. *JAMA Neurol.* 71, 505–508. doi: 10.1001/jamaneurol.2013.5847 1209
- 1161 Brunoni, A. R., Baeken, C., Machado-Vieira, R., Gattaz, W. F., and Vanderhasselt,
1162 M. A. (2015). BDNF blood levels after non-invasive brain stimulation
1163 interventions in major depressive disorder: a systematic review and meta-
1164 analysis. *World J. Biol. Psychiatry* 16, 114–122. doi: 10.3109/15622975.2014.
1165 958101 1210
- 1165 Chakraborty, S., Hill, E. S., Christian, D. T., Helfrich, R., Riley, S., Schneider, C.,
1166 et al. (2019). Reduced presynaptic vesicle stores mediate cellular and network
1167 plasticity defects in an early-stage mouse model of Alzheimer's disease. *Mol.*
1168 *Neurodegener.* 14:7. doi: 10.1186/s13024-019-0307-7 1211
- 1168 Cocco, S., Podda, M. V., and Grassi, C. (2018). Role of BDNF signaling in
1169 memory enhancement induced by transcranial direct current stimulation.
1170 *Front. Neurosci.* 12:427. doi: 10.3389/fnins.2018.00427 1212
- 1171 Cohen, S. J., and Stackman, R. W. Jr. (2015). Assessing rodent hippocampal
1172 involvement in the novel object recognition task: a review. *Behav. Brain Res.*
1173 285, 105–117. doi: 10.1016/j.bbr.2014.08.002 1213
- 1173 Del Prete, D., Checler, F., and Chami, M. (2014). Ryanodine receptors:
1174 physiological function and deregulation in Alzheimer disease. *Mol.*
1175 *Neurodegener.* 9:21. doi: 10.1186/1750-1326-9-21 1214
- 1175 Fà, M., Puzzo, D., Piacentini, R., Staniszewski, A., Zhang, H., Baltrons, M. A., et al.
1176 (2016). Extracellular tau oligomers produce an immediate impairment of LTP
1177 and memory. *Sci. Rep.* 6:19393. doi: 10.1038/srep19393 1215
- 1177 Franklin, K. B. J., and Paxinos, G. T. (1997). *The Mouse Brain in Stereotaxic*
1178 *Coordinates*. New York, NY: Academic Press. 1216
- 1178 Fusco, S., Spinelli, M., Cocco, S., Ripoli, C., Mastrodonato, A., Natale, F.,
1179 et al. (2019). Maternal insulin resistance multigenerationally impairs synaptic
1180 plasticity and memory via gametic mechanisms. *Nat. Commun.* 10:4799. doi:
1181 10.1038/s41467-019-12793-3 1217
- 1181 Galluzzi, S., Marizzoni, M., Babiloni, C., Albani, D., Antelmi, L., Bagnoli, C., et al.
1182 (2016). Clinical and biomarker profiling of prodromal Alzheimer's disease in
1183 workpackage 5 of the Innovative Medicines Initiative PharmaCog project: a
1184 'European ADNI study'. *J. Intern. Med.* 279, 576–591. doi: 10.1111/joim.12482 1218
- 1184 Gondard, E., Soto-Montenegro, M. L., Cassol, A., Lozano, A. M., and Hamani,
1185 C. (2019). Transcranial direct current stimulation does not improve memory
1186 deficits or alter pathological hallmarks in a rodent model of Alzheimer's disease.
1187 *J. Psychiatr. Res.* 114, 93–98. doi: 10.1016/j.jpsychires.2019.04.016 1219
- 1187 Gulisano, W., Maugeri, D., Baltrons, M. A., Fà, M., Amato, A., Palmeri, A., et al.
1188 (2018a). Role of amyloid- β and tau proteins in Alzheimer's disease: confuting
1189 the amyloid cascade. *J. Alzheimers Dis.* 64, S611–S631. doi: 10.3233/JAD-
1190 179935 1220
- 1189 Gulisano, W., Melone, M., Li Puma, D. D., Tropea, M. R., Palmeri, A., Arancio,
1190 O., et al. (2018b). The effect of amyloid- β peptide on synaptic plasticity and
1191 memory is influenced by different isoforms, concentrations and aggregation
1192 status. *Neurobiol. Aging* 71, 51–60. doi: 10.1016/j.neurobiolaging.2018.06.025 1221
- 1192 Irvine, G. B., El-Agnaf, O. M., Shankar, G. M., and Walsh, D. M. (2008). Protein
1193 aggregation in the brain: the molecular basis for Alzheimer's and Parkinson's
1194 diseases. *Mol. Med.* 14, 451–464. doi: 10.2119/2007-00100 1222
- 1194 Jackson, M. P., Rahman, A., Lafon, B., Kronberg, G., Ling, D., Parra, L. C., et al.
1195 (2016). Animal models of transcranial direct current stimulation: methods and
1196 mechanisms. *Clin. Neurophysiol.* 127, 3425–3454. doi: 10.1016/j.clinph.2016.08.
1197 016 1223
- 1196 Jackson, M. P., Truong, D., Brownlow, M. L., Wagner, J. A., McKinley, R. A.,
1197 Bikson, M., et al. (2017). Safety parameter considerations of anodal transcranial
1198 direct current stimulation in rats. *Brain Behav. Immun.* 64, 152–161. doi: 10.
1199 1016/j.bbi.2017.04.008 1224
- 1197 Joe, E., and Ringman, J. M. (2019). Cognitive symptoms of Alzheimer's disease:
1198 clinical management and prevention. *BMJ* 367:l6217. doi: 10.1136/bmj.l6217 1225
- 1198 Joseph, D. J., Liu, C., Peng, J., Liang, G., and Wei, H. (2019). Isoflurane
1199 mediated neuropathological and cognitive impairments in the triple transgenic
1200 Alzheimer's mouse model are associated with hippocampal synaptic deficits in
1201 an age-dependent manner. *PLoS One* 14:e0223509. doi: 10.1371/journal.pone.
1202 0223509 1226
- 1200 Kim, M. S., Koo, H., Han, S. W., Paulus, W., Nitsche, M. A., Kim, Y. H., et al.
1201 (2017). Repeated anodal transcranial direct current stimulation induces neural
1202 plasticity-associated gene expression in the rat cortex and hippocampus. *Restor.*
1203 *Neurol. Neurosci.* 35, 137–146. doi: 10.3233/RNN-160689 1227
- 1203 Kopeikina, K. J., Hyman, B. T., and Spire-Jones, T. L. (2012). Soluble forms of
1204 tau are toxic in Alzheimer's disease. *Transl Neurosci.* 3, 223–233. doi: 10.2478/
1205 s13380-012-0032-y 1228
- 1204 Kronberg, G., Rahman, A., Sharma, M., Bikson, M., and Parra, L. C. (2020). Direct
1205 current stimulation boosts hebbian plasticity in vitro. *Brain Stimul.* 13, 287–301.
1206 doi: 10.1016/j.brs.2019.10.014 1229
- 1205 Lashley, T., Schott, J. M., Weston, P., Murray, C. E., Wellington, H., Keshavan,
1206 A., et al. (2018). Molecular biomarkers of Alzheimer's disease: progress and
1207 prospects. *Dis. Model. Mech.* 11:dmm031781. doi: 10.1242/dmm.031781 1230
- 1206 Laske, C., Stransky, E., Leyhe, T., Eschweiler, G. W., Wittorf, A., Richartz, E., et al.
1207 (2006). Stage-dependent BDNF serum concentrations in Alzheimer's disease.
1208 *J. Neural Transm.* 113, 1217–1224. doi: 10.1007/s00702-005-0397-y 1231
- 1207 Leone, L., Colussi, C., Gironi, K., Longo, V., Fusco, S., Li Puma, D. D., et al. (2019).
1208 Altered Nup153 expression impairs the function of cultured hippocampal
1209 neural stem cells isolated from a mouse model of Alzheimer's disease. *Mol.*
1210 *Neurobiol.* 56, 5934–5949. doi: 10.1007/s12035-018-1466-1 1232
- 1208 Li, T., Jiao, J. J., Hölscher, C., Wu, M. N., Zhang, J., Tong, J. Q., et al. (2018).
1209 A novel GLP-1/GIP/Gcg triagonist reduces cognitive deficits and pathology
1210 in the 3xTg mouse model of Alzheimer's disease. *Hippocampus* 28, 358–372.
1211 doi: 10.1002/hipo.22837 1233
- 1209 Merlo, S., Spampinato, S. F., and Sortino, M. A. (2019). Early compensatory
1210 responses against neuronal injury: a new therapeutic window of opportunity
1211 for Alzheimer's disease? *CNS Neurosci. Ther.* 25, 5–13. doi: 10.1111/cns.13050 1234
- 1210 Naegelin, Y., Dingsdale, H., Säuberli, K., Schädelin, S., Kappos, L., and Barde,
1211 Y. A. (2018). Measuring and validating the levels of brain-derived neurotrophic
1212 factor in human serum. *eNeuro* 5:ENEURO.0419-17.2018. doi: 10.1523/
1213 ENEURO.0419-17.2018 1235
- 1211 Nelson, O., Supnet, C., Liu, H., and Bezprozvanny, I. (2010). Familial Alzheimer's
1212 disease mutations in presenilins: effects on endoplasmic reticulum calcium
1213 homeostasis and correlation with clinical phenotypes. *J. Alzheimers Dis.* 21,
1214 781–793. doi: 10.3233/JAD-2010-100159 1236
- 1212 Oddo, S., Caccamo, A., Shepherd, J. D., Murphy, M. P., Golde, T. E., Kaye,
1213 R., et al. (2003). Triple-transgenic model of Alzheimer's disease with plaques
1214 and tangles: intracellular A β and synaptic dysfunction. *Neuron* 39, 409–421.
1215 doi: 10.1016/S0896-6273(03)00434-3 1237
- 1213 Paciello, F., Podda, M. V., Rolesi, R., Cocco, S., Petrosini, L., Troiani, D., et al.
1214 (2018). Anodal transcranial direct current stimulation affects auditory cortex
1215 plasticity in normal-hearing and noise-exposed rats. *Brain Stimul.* 11, 1008–
1216 1023. doi: 10.1016/j.brs.2018.05.017 1238
- 1214 Pelletier, S. J., and Cicchetti, F. (2014). Cellular and molecular mechanisms of
1215 action of transcranial direct current stimulation: evidence from in vitro and
1216 in vivo models. *Int. J. Neuropsychopharmacol.* 18:yu047. doi: 10.1093/ijnp/
1217 pyu047 1239
- 1215 Podda, M. V., Cocco, S., Mastrodonato, A., Fusco, S., Leone, L., Barbati, S. A., et al.
1216 (2016). Anodal transcranial direct current stimulation boosts synaptic plasticity
1217 1250

- 1255 and memory in mice via epigenetic regulation of Bdnf expression. *Sci. Rep.* 6:22180. doi: 10.1038/srep22180
- 1256
- 1257 Podda, M. V., D'Ascenzo, M., Leone, L., Piacentini, R., Azzena, G. B., and Grassi, C. (2008). Functional role of cyclic nucleotide-gated channels in rat medial vestibular nucleus neurons. *J. Physiol.* 586, 803–815. doi: 10.1113/jphysiol.2007.146019
- 1258
- 1259
- 1260 Podda, M. V., Leone, L., Barbati, S. A., Mastrodonato, A., Li Puma, D. D., and Piacentini, R. (2014). Extremely low-frequency electromagnetic fields enhance the survival of newborn neurons in the mouse hippocampus. *Eur. J. Neurosci.* 39, 893–903. doi: 10.1111/ejn.12465
- 1261
- 1262
- 1263 Puzzo, D., Piacentini, R., Fà, M., Gulisano, W., Li Puma, D. D., Staniszewski, A., et al. (2017). LTP and memory impairment caused by extracellular A β and Tau oligomers is APP-dependent. *eLife* 6:e26991. doi: 10.7554/eLife.26991
- 1264
- 1265
- 1266 Rahman, A., Lafon, B., Parra, L. C., and Bikson, M. (2017). Direct current stimulation boosts synaptic gain and cooperativity in vitro. *J. Physiol.* 595, 3535–3547. doi: 10.1113/JP273005
- 1267
- 1268 Rajji, T. K. (2019a). Impaired brain plasticity as a potential therapeutic target for treatment and prevention of dementia. *Expert. Opin. Ther. Targets* 23, 21–28. doi: 10.1080/14728222.2019.1550074
- 1269
- 1270
- 1271 Rajji, T. K. (2019b). Transcranial magnetic and electrical stimulation in alzheimer's disease and mild cognitive impairment: a review of randomized controlled trials. *Clin. Pharmacol. Ther.* 106, 776–780. doi: 10.1002/cpt.1574
- 1272
- 1273 Ranieri, F., Podda, M. V., Riccardi, E., Frisullo, G., Dileone, M., and Profice, P. (2012). Modulation of LTP at rat hippocampal CA3-CA1 synapses by direct current stimulation. *J. Neurophysiol.* 107, 1868–1880. doi: 10.1152/jn.00319.2011
- 1274
- 1275
- 1276 Ripoli, C., Cocco, S., Li Puma, D. D., Piacentini, R., Mastrodonato, A., Scala, F., et al. (2014). Intracellular accumulation of amyloid- β (A β) protein plays a major role in A β -induced alterations of glutamatergic synaptic transmission and plasticity. *J. Neurosci.* 34, 12893–12903. doi: 10.1523/jneurosci.1201-14.2014
- 1277
- 1278
- 1279 Rohan, J. G., Carhuatanta, K. A., McInturf, S. M., Miklasevich, M. K., and Jankord, R. (2015). Modulating hippocampal plasticity with in vivo brain stimulation. *J. Neurosci.* 35, 12824–12832. doi: 10.1523/JNEUROSCI.2376-15.2015
- 1280
- 1281
- 1282 Serrano-Pozo, A., Frosch, M. P., Masliah, E., and Hyman, B. T. (2011). Neuropathological alterations in Alzheimer disease. *Cold Spring Harb. Perspect. Med.* 1:a006189. doi: 10.1101/cshperspect.a006189
- 1283
- 1284
- 1285 Shi, M., Kovac, A., Korff, A., Cook, T. J., Ginghina, C., Bullock, K. M., et al. (2016). CNS tau efflux via exosomes is likely increased in Parkinson's disease but not in Alzheimer's disease. *Alzheimers Dement.* 12, 1125–1131. doi: 10.1016/j.jalz.2016.04.003
- 1286
- 1287
- 1288
- 1289
- 1290
- 1291
- 1292
- 1293
- 1294
- 1295
- 1296
- 1297
- 1298
- 1299
- 1300
- 1301
- 1302
- 1303
- 1304
- 1305
- 1306
- 1307
- 1308
- 1309
- 1310
- 1311
- Shipton, O. A., El-Gaby, M., Apergis-Schoute, J., Deisseroth, K., Bannerman, D. M., Paulsen, O., et al. (2014). Left-right dissociation of hippocampal memory processes in mice. *Proc. Natl. Acad. Sci. U.S.A.* 111, 15238–15243. doi: 10.1073/pnas.1405648111
- 1312
- 1313
- 1314
- 1315
- 1316
- 1317
- 1318
- 1319
- 1320
- 1321
- 1322
- 1323
- 1324
- 1325
- 1326
- 1327
- 1328
- 1329
- 1330
- 1331
- 1332
- 1333
- 1334
- 1335
- 1336
- 1337
- 1338
- 1339
- 1340
- 1341
- 1342
- 1343
- 1344
- 1345
- 1346
- 1347
- 1348
- 1349
- 1350
- 1351
- 1352
- 1353
- 1354
- 1355
- 1356
- 1357
- 1358
- 1359
- 1360
- 1361
- 1362
- 1363
- 1364
- 1365
- 1366
- 1367
- 1368
- Stafford, J., Brownlow, M. L., Qualley, A., and Jankord, R. (2018). AMPA receptor translocation and phosphorylation are induced by transcranial direct current stimulation in rats. *Neurobiol. Learn. Mem.* 150, 36–41. doi: 10.1016/j.nlm.2017.11.002
- Stover, K. R., Campbell, M. A., Van Winssen, C. M., and Brown, R. E. (2015). Early detection of cognitive deficits in the 3xTg-AD mouse model of Alzheimer's disease. *Behav. Brain Res.* 289, 29–38. doi: 10.1016/j.bbr.2015.04.012
- Vecchio, F., Miraglia, F., Iberite, F., Lacidogna, G., Guglielmi, V., Marra, C., et al. (2018). Sustainable method for Alzheimer dementia prediction in mild cognitive impairment: electroencephalographic connectivity and graph theory combined with apolipoprotein E. *Ann. Neurol.* 84, 302–314. doi: 10.1002/ana.25289
- Vorhees, C. V., and Williams, M. T. (2014). Assessing spatial learning and memory in rodents. *ILAR J.* 55, 310–332. doi: 10.1093/ilar/ilu013
- Whitcomb, D. J., Hogg, E. L., Regan, P., Piers, T., Narayan, P., Whitehead, G., et al. (2015). Intracellular oligomeric amyloid-beta rapidly regulates GluA1 subunit of AMPA receptor in the hippocampus. *Sci. Rep.* 9:10934. doi: 10.1038/srep10934
- Yu, T. H., Wu, Y. J., Chien, M. E., and Hsu, K. S. (2019). Transcranial direct current stimulation induces hippocampal metaplasticity mediated by brain-derived neurotrophic factor. *Neuropharmacology* 144, 358–367. doi: 10.1016/j.neuropharm.2018.11.012

Conflict of Interest: The authors declare that the research was conducted in the absence of any commercial or financial relationships that could be construed as a potential conflict of interest.

Copyright © 2020 Cocco, Rinaudo, Fusco, Longo, Gironi, Renna, Aceto, Mastrodonato, Li Puma, Podda and Grassi. This is an open-access article distributed under the terms of the Creative Commons Attribution License (CC BY). The use, distribution or reproduction in other forums is permitted, provided the original author(s) and the copyright owner(s) are credited and that the original publication in this journal is cited, in accordance with accepted academic practice. No use, distribution or reproduction is permitted which does not comply with these terms.